American Journal of Geriatric Psychiatry

Post-mortem cortical transcriptomics of Lewy body dementia reveal mitochondrial dysfunction and lack of neuroinflammation

--Manuscript Draft--

Manuscript Number:	AMGP-19-115R2
Full Title:	Post-mortem cortical transcriptomics of Lewy body dementia reveal mitochondrial dysfunction and lack of neuroinflammation
Article Type:	Regular Research Article
Keywords:	Lewy body dementia; High-Throughput RNA sequencing; Systems biology; Parkinson disease; Mitochondria
Corresponding Author:	Anto P. Rajkumar, M.D., D.N.B., M.R.C.Psych., Ph.D, Ph.D. Institute of Psychiatry, Psychology, & Neuroscience, King's College, London, UK London, UNITED KINGDOM
Corresponding Author Secondary Information:	
Corresponding Author's Institution:	Institute of Psychiatry, Psychology, & Neuroscience, King's College, London, UK
Corresponding Author's Secondary Institution:	
First Author:	Anto P. Rajkumar, M.D., D.N.B., M.R.C.Psych., Ph.D, Ph.D.
First Author Secondary Information:	
Order of Authors:	Anto P. Rajkumar, M.D., D.N.B., M.R.C.Psych., Ph.D, Ph.D.
	Gholamreza Bidkhori, Ph.D.
	Saeed Shoaie, Ph.D.
	Emily Clarke, Ph.D.
	Hamilton Morrin
	Abdul Hye, Ph.D.
	Gareth Williams, Ph.D.
	Clive Ballard, M.D., Ph.D.
	Paul Francis, Ph.D.
	Dag Aarsland, M.D., Ph.D.
Manuscript Region of Origin:	UNITED KINGDOM
Abstract:	Objectives Prevalence of Lewy body dementias (LBD) is second only to Alzheimer's disease (AD) among people with neurodegenerative dementia. LBD cause earlier mortality, more intense neuropsychiatric symptoms, more caregivers' burden, and higher costs than AD. The molecular mechanisms underlying LBD are largely unknown. As advancing molecular level mechanistic understanding is essential for identifying reliable peripheral biomarkers and novel therapeutic targets for LBD, we aimed to identify differentially expressed genes (DEG), and dysfunctional molecular networks in post-mortem LBD brains. Methods We investigated the transcriptomics of post-mortem anterior cingulate and dorsolateral prefrontal cortices of people with pathology-verified LBD using next-generation RNA-sequencing. We verified the identified DEG using high-throughput quantitative polymerase chain reactions. Functional implications of identified DEG, and the

	consequent metabolic reprogramming were evaluated by Ingenuity pathway analyses, genome-scale metabolic modelling, reporter metabolite analyses, and in-silico gene silencing. Results We identified and verified 12 novel DEGs (MPO, SELE, CTSG, ALPI, ABCA13, GALNT6, SST, RBM3, CSF3, SLC4A1, OXTR, and RAB44) in LBD brains with genome-wide statistical significance. We documented statistically significant downregulation of several cytokine genes. Identified dysfunctional molecular networks highlighted the contributions of mitochondrial dysfunction, oxidative stress, and immunosenescence towards neurodegeneration in LBD. Conclusion Our findings support that chronic microglial activation and neuroinflammation, well-documented in AD, are notably absent in LBD. The lack of neuroinflammation in LBD brains were corroborated by statistically significant downregulation of several inflammatory markers. Identified DEGs, especially downregulated inflammatory markers, may aid distinguishing LBD from AD, and their biomarker potential warrant further investigation.
Additional Information:	
Question	**Response**
Please provide the word count for your submission. The word count applies to only the main manuscript text; it should not include the abstract, references, figure legends, or tables.	3301
Please indicate the number of figures, if any, that are included with this submission.	2
Please indicate the number of tables, if any, that are included with this submission.	2

Highlights

What is the primary question addressed by this study?

What are the differentially expressed genes and dysfunctional molecular networks in post-mortem brains of people with Lewy body dementia (LBD)?

What is the main finding of this study?

This study has identified and verified 12 novel differentially expressed genes in LBD brains. Downregulation of several inflammatory markers revealed the absence of chronic neuroinflammation in LBD.

What is the meaning of the finding?

The findings advance molecular level mechanistic understanding and indicate potential biomarkers for LBD that warrant further investigation.

Article type: Regular research article

Title: Post-mortem cortical transcriptomics of Lewy body dementia reveal mitochondrial dysfunction and lack of neuroinflammation

Authors and affiliations:

1. Anto P. Rajkumar [a,b], MD, MRCPsych, PhD, PhD,
2. Gholamreza Bidkhori [c], PhD,
3. Saeed Shoaie [c], PhD,
4. Emily Clarke [d], PhD,
5. Hamilton Morrin [e],
6. Abdul Hye [a,f], PhD,
7. Gareth Williams [d], PhD,
8. Clive Ballard [a,g], MD,
9. Paul Francis [a,d], PhD,
10. Dag Aarsland [a,b] MD, PhD

[a] Department of Old Age Psychiatry, Institute of Psychiatry, Psychology, & Neuroscience, King's College London, 16, De Crespigny Park, London-SE5 8AF, United Kingdom (UK)

[b] Mental Health of Older Adults and Dementia Clinical Academic Group, South London and Maudsley NHS foundation Trust, 115, Denmark Hill, London-SE5 8AQ, UK

[c] Centre for Host–Microbiome Interactions, Faculty of Dentistry, Oral & Craniofacial Sciences, King's College London, London, SE1 9RT, UK

[d] Wolfson Centre for Age-Related Diseases, King's College London, London-SE11UL, UK

[e] Guy's hospital, King's College London, Great Maze Pond, London-SE1 9RT, UK

[f] NIHR Biomedical Research Centre for Mental Health and Biomedical Research Unit for Dementia at South London and Maudsley NHS foundation trust, London- SE5 9RT, UK

[g] The Medical School, Exeter University, Heavitree Road, Exeter-EX1 2LU, UK

Corresponding author:

Dr. Anto Praveen Rajkumar, M.D., D.N.B., M.R.C.Psych., Ph.D., Ph.D.,

Academic Clinical Lecturer, Department of Old Age Psychiatry,

Institute of Psychiatry, Psychology, & Neuroscience,

King's College London,

16, De Crespigny Park,

London - SE5 8AF, United Kingdom.

Phone: +44 02078480508

Email: Anto.Rajamani@kcl.ac.uk

Word counts : For abstract : 245

For Text : 3301

Number of Tables : Two

Number of Figures : Two

Supplemental digital content : 15

Abstract:

Objectives: Prevalence of Lewy body dementias (LBD) is second only to Alzheimer's disease (AD) among people with neurodegenerative dementia. LBD cause earlier mortality, more intense neuropsychiatric symptoms, more caregivers' burden, and higher costs than AD. The molecular mechanisms underlying LBD are largely unknown. As advancing molecular level mechanistic understanding is essential for identifying reliable peripheral biomarkers and novel therapeutic targets for LBD, we aimed to identify differentially expressed genes (DEG), and dysfunctional molecular networks in post-mortem LBD brains.

Methods: We investigated the transcriptomics of post-mortem anterior cingulate and dorsolateral prefrontal cortices of people with pathology-verified LBD using next-generation RNA-sequencing. We verified the identified DEG using high-throughput quantitative polymerase chain reactions. Functional implications of identified DEG, and the consequent metabolic reprogramming were evaluated by Ingenuity pathway analyses, genome-scale metabolic modelling, reporter metabolite analyses, and *in-silico* gene silencing.

Results: We identified and verified 12 novel DEGs (*MPO*, *SELE*, *CTSG*, *ALPI*, *ABCA13*, *GALNT6*, *SST*, *RBM3*, *CSF3*, *SLC4A1*, *OXTR*, and *RAB44*) in LBD brains with genome-wide statistical significance. We documented statistically significant downregulation of several cytokine genes. Identified dysfunctional molecular networks highlighted the contributions of mitochondrial dysfunction, oxidative stress, and immunosenescence towards neurodegeneration in LBD.

Conclusion: Our findings support that chronic microglial activation and neuroinflammation, well-documented in AD, are notably absent in LBD. The lack of neuroinflammation in LBD brains were corroborated by statistically significant downregulation of several inflammatory markers. Identified DEGs, especially downregulated inflammatory markers, may aid distinguishing LBD from AD, and their biomarker potential warrant further investigation.

Key words: Lewy body dementia; High-Throughput RNA sequencing; Systems biology; Parkinson disease; Mitochondria

Introduction:

Lewy body dementia (LBD) is a major public health problem worldwide. Prevalence of Lewy body dementia (LBD) is second only to Alzheimer's disease (AD) among people with neurodegenerative dementia (1). LBD cause earlier mortality (2), earlier nursing home admissions, poorer quality-of-life, higher costs (3), more frequent falls, and more caregivers' burden than AD. LBD include two overlapping clinical syndromes, dementia with Lewy bodies (DLB) and Parkinson's disease (PD) dementia (PDD). They cause more frequent and more intense neuropsychiatric symptoms including visual hallucinations, delusions, agitation, and depression than AD (4). Antipsychotic medications should be avoided in all people with dementia whenever possible, and there is an urgent clinical need for diagnosing LBD early, because treating neuropsychiatric symptoms, common in LBD, with any antipsychotic medication risks potentially fatal adverse effects in people with LBD (5). However, the molecular mechanisms underlying neurodegeneration in LBD remain largely unknown, and prior research that focused mainly on known AD and PD biomarkers have not identified any reliable genetic markers for LBD (6). Moreover, there are no disease-modifying treatment for LBD (7). Hence, advancing molecular level mechanistic understanding is urgently needed for facilitating discovery of multimodal biomarkers and novel therapeutic targets for LBD (7,8).

A few candidate-gene association studies and a genome-wide association study (GWAS) have associated LBD with polymorphisms in *APOE*, *SNCA*, *GBA*, *STX1B*, *GABRB3*, *CNTN1*, and *SCARB2* (9-11), but they could not ascertain functional implications of identified genetic associations. As a definite DLB diagnosis can be confirmed only by post-mortem (12),

genetic studies investigating people living with LBD are prone for misclassification bias. Hence, transcriptomic studies that identify differentially expressed ribonucleic acids (RNA) in post-mortem LBD brains are essential for understanding functionally relevant gene expression changes, and their dysfunctional molecular networks (13-15). Moreover, further research on the transcriptomics of LBD brains is needed for clarifying their neuroimmunology. Chronic microglial activation and neuroinflammation contribute to neurodegeneration in AD (16), but recent immunohistochemical studies have documented absence of neuroinflammation in LBD (17,18). Immunosenescence and consequent impaired neuronal survival are hypothesized to contribute to LBD pathology (17,18). Hence, we aimed to identify differentially expressed genes (DEG), dysfunctional molecular networks, and metabolic reprogramming in post-mortem anterior cingulate (ACC), and dorsolateral prefrontal (DLPFC) cortices of people with pathology-verified LBD.

Methods:

Post-mortem brain tissue:

The Brains for Dementia Research (BDR) network of brain banks (19), UK, provided necessary post-mortem brain tissue, and ethical approval for this study. We obtained frozen sections of ACC (Brodmann area 24), and DLPFC (Brodmann area 9) of people with pathology-verified DLB (n=7), PDD (n=7), and of older people without dementia or PD (NDC) (n=7). The groups did not differ significantly on their age ($F=0.88;df=2,18;p=0.43$), and on their post-mortem intervals ($F=0.04;df=2,18;p=0.96$). We could not get ACC tissue of one person with DLB, and DLPFC tissue of one NDC person was not available (Supplemental digital content (SDC)-1). ACC is known to have high levels of Lewy body pathology in LBD (15), and Lewy body densities in ACC can predict cognitive impairment in PD (20). People with DLB have greater impairment of executive functions, regulated by DLPFC, than people with AD (21). Hence, we investigated the transcriptomics of these two cortical regions.

RNA extraction:

50mg of brain tissue per sample were excised on dry ice. Excised tissue was homogenized using the T10-basic ultra-turrax, and disposable dispersing element S10D-7G-KS-110 (Ika works, Wilmington, USA). Total RNA was extracted using the RNeasy plus universal mini kit (Qiagen, Hilden, Germany). Quantity and quality of RNA were assessed using the NanoDrop ND-1000 (Thermo Fisher Scientific, Waltham, USA). Mean 260/280 and 260/230 spectrophotometer absorbance ratios of purified RNA were 2.06 (95%CI 2.05-2.07), and 1.56 (95%CI 1.48-1.64), respectively.

Next-generation RNA-sequencing (RNA-Seq):

cDNA libraries were prepared from RNA samples using TruSeq RNA sample preparation kit (Illumina, San Diego, USA). The cDNA libraries underwent paired-end sequencing (75 base pairs/read) using the Illumina HiSeq-4000 (Illumina, San Diego, USA) in the Wellcome Centre for Human Genetics (WHG), Oxford, UK. We obtained a minimum of 30 million clean reads/sample.

RNA-Seq data analyses:

RNA-Seq reads passed quality control, if they did not include any ambiguous bases, and if more than 90% of bases had less than 1% sequencing error. Such reads were aligned to the human genome (Homo_sapiens.GRCh38) with corresponding gene model annotation (Homo_sapiens.GRCh38.88.gtf) using the *HISAT2* (22). Aligned reads were counted using the *featureCounts* (23) (SDC-2; SDC-3). DEGs were identified by a previously experimentally validated (24) *edgeR* 3.18.1 algorithm employing tag-wise dispersion (25), and Benjamini-Hochberg genome-wide false discovery rate (FDR) correction (5%). The *edgeR* algorithm calculated p-values by employing exact tests (no df) after fitting gene-specific quasi-negative binominal models and estimating dispersion using the quantile adjusted conditional maximum likelihood method. The LBD group including both DLB and PDD groups (n=14) was compared

with the NDC group for identifying DEGs in LBD brains. Later, pairwise subgroup analyses were conducted with FDR correction.

Verification of identified DEGs:

Differential expression of 78 selected genes (SDC-4) including all protein coding FDR-adjusted DEGs and 10 randomly selected DEGs (*edgeR* $p<0.05$; no df) in DLPFC of LBD brains were evaluated using high-throughput quantitative polymerase chain reactions (qPCR). One µg of RNA per sample from the aliquots of RNA that had been sequenced (N=40) were reverse transcribed using the iScript™ advanced cDNA synthesis kit (Bio-Rad, Hercules, USA). After 14 cycles of specific target amplification with the PreAmp master-mix (Fluidigm, San Francisco, USA), high-throughput qPCR was performed using the BioMark HD, GE 96.96 dynamic arrays (Fluidigm, San Francisco, USA), and SsoFast EvaGreen low ROX kit (Bio-Rad, Hercules, USA) (SDC-5). Verification of differential expression of a gene was defined by the following criteria (26), (i) Both RNA-seq and qPCR showed same direction of differential expression, (ii) Differential expression fold change, estimated by qPCR, was either above 1.25 or below 0.80 (logarithmic cut-off was ±0.3219).

Ingenuity Pathway Analysis (IPA):

Functional implications of identified DEGs (*edgeR* $p<0.05$; no df) were analyzed by the IPA using the Ingenuity knowledge base (Ingenuity, Redwood City, USA). The IPA helps identifying potential biomarkers within the context of biological systems. Our analysis settings included stringent filters with only experimentally observed relationships, and we identified dysfunctional molecular networks in LBD brains.

Comparison with AD gene expression data:

We gathered all AD related gene expression data publicly available in the NCBI GEO database (27). A DEG was deemed to be specific to LBD, if the gene either was not altered in the AD gene expression profiles, or if it was reportedly altered in the opposite direction.

Brain-specific genome-scale metabolic model (GEM):

We used a previously generated brain-specific GEM (28). The GEM includes 630 metabolic reactions, controlled by 570 genes, within and between astrocytes and neurons, and the metabolites that exchange or transport through the blood-brain barrier. We have modified the lactate release from neurons, glycogen accumulation in astrocytes, glutamate cycling, GABA transfer direction, and pentose phosphate pathway, and have included the reaction of astrocyte lactate shuttle to the GEM based on our transcriptomic data. Glutamate/glutamine cycle and ATP demand were considered as objective functions. In order to generate tissue-specific GEMs, we employed Metabolic Adjustment by Differential Expression (MADE) (29) and Toolbox for Integrating Genome scale metabolism, Expression, and Regulation (TIGER) (30) using logarithmic fold changes and p-values, obtained from the *edgeR* (25) analyses, as input. Flux balance analysis (FBA) was used as a mathematical constraint-based modelling approach for analyzing the flow of metabolites through a metabolic network, and it investigated the metabolic reprogramming in LBD brains.

Reporter metabolite analyses:

We further investigated the metabolic reprogramming in LBD brains by reporter metabolite analyses using an updated human metabolic reactions model (31), the Platform for Integrated Analysis of Omics data (PIANO) (32), and gene-level logarithmic fold changes and the p-values, obtained from the *edgeR* analyses, with the Stouffer's test (no df) employing a permutation (1000) approach.

***In-silico gene silencing*:**

The effects of silencing each of the 570 metabolic genes was simulated using the generated GEMs by removing reaction(s) associated with the gene. The reactions were retained, if another gene catalyzing the same reaction(s) is present. Then, FBA was performed for checking the effects of *in-silico* gene silencing on the functionality of models. When the

gene silencing decreased the flux of objective function, it was considered as an essential gene for that condition.

Results:

DEGs in LBD brains:

The LBD (DLB and PDD) and NDC groups did not differ significantly on their spectrophotometer mean absorbance ratios in both ACC (260/280 (t=0.74;df=18;p=0.47); 260/230 (t=-2.02;df=18;p=0.06)) and DLPFC (260/280 (t=0.21;df=18;p=0.84); 260/230 (t=1.48;df=18;p=0.16)). We identified 1464 upregulated, and 1652 downregulated DEGs (*edgeR* $p<0.05$; no df) in ACC (SDC-6), and 1233 upregulated and 1414 downregulated DEGs (*edgeR* $p<0.05$; no df) in DLPFC (SDC-7) of LBD brains, compared to NDC brains. After genome-wide FDR correction, we identified 12 protein coding DEGs in LBD brains (Table-1). *MPO*, *SELE*, *CTSG*, *ALPI*, and *ABCA13* were significantly downregulated in both ACC and DLPFC. *GALNT6* was significantly upregulated in DLPFC. *RBM3*, *CSF3*, *SLC4A1*, *OXTR*, and *RAB44* were significantly downregulated in ACC, and *SST* was significantly downregulated in DLPFC of LBD brains. Differential expression levels of these 12 DEGs could be verified (26) by high-throughput qPCR (Table-1). Moreover, differential expression levels of 62.3% (38/61; 95%CI 50.1-74.5%) of other DEGs (*edgeR* $p<0.05$; no df) could be verified (26) by high-throughput qPCR (SDC-8). Cytokine gene *IL1B*, chemokine gene *CXCL11*, and neutrophil defensin genes, *DEFA3* and *DEFA4*, were significantly downregulated (*edgeR* $p<0.05$; no df) in both ACC and DLPFC of LBD brains, and their differential expression levels could be verified by qPCR in both cortical regions. The statistically significant (*edgeR* $p<0.05$; no df) downregulated DEGs in LBD brains, verified by high-throughput qPCR, included *VGF* encoding a nerve growth factor, *VCAM1* encoding a vascular cell adhesion molecule, and *STX11* encoding a syntaxin (Table-2).

DEGs in DLB and PDD brains:

The subgroup analyses identified 735 upregulated, and 979 downregulated DEGs (*edgeR* $p<0.05$; no df) in ACC, and 973 upregulated and 1330 downregulated DEGs (*edgeR* $p<0.05$; no df) in DLPFC of DLB brains, compared to NDC brains (SDC-9). After FDR correction, *CTSG*, and *SELE* were significantly downregulated, and *GIPR*, and *PSPHP1* were significantly upregulated in DLPFC of DLB brains. There was not any FDR-adjusted DEG in ACC of DLB brains. When we compared PDD brains with NDC brains, we identified 1764 upregulated, and 2066 downregulated DEGs (*edgeR* $p<0.05$; no df) in ACC, and 1293 upregulated and 1114 downregulated DEGs (*edgeR* $p<0.05$; no df) in DLPFC of PDD brains (SDC-10). *ADAMTS2* was significantly upregulated, and *MPO*, and *OXTR*, were significantly downregulated in ACC, as well as *GALNT6* was significantly upregulated, and *CTSG*, *SST*, and *OR11H4* were significantly downregulated in DLPFC of PDD brains, compared to NDC, after FDR correction (SDC-10). While comparing with PDD brains, there were 1236 downregulated and 1043 upregulated DEGs (*edgeR* $p<0.05$; no df) in ACC of DLB brains, but none of them was significant after FDR correction. We identified 607 upregulated and 987 downregulated DEGs (*edgeR* $p<0.05$; no df) in DLPFC of DLB brains, compared to PDD brains. DLB could be differentiated from PDD by the downregulation of nine FDR-adjusted DEGs including *PTGER3*, and *CRABP1* in their DLPFC (SDC-11) (SDC-12).

Dysfunctional molecular networks:

The genes, associated with the agranulocytes adhesion and diapedesis, granulocytes adhesion and diapedesis, atherosclerosis signaling, and differential regulation of cytokine production in macrophages and T-helper cells by IL-17A and IL-17F pathways, were significantly enriched among the DEGs (*edgeR* $p<0.05$; no df) in both cortical regions of LBD brains after Benjamini-Hochberg FDR correction (Figure-1A&1B). Immune system related canonical pathways including IL-6 signaling, systemic lupus erythematosus signaling,

communication between innate and adaptive immune cells, and role of cytokines in mediating communication between immune cells were significantly enriched among the DEGs in DLPFC of LBD brains after FDR correction (Figure-1A). Downregulation of genome-wide significant DEGs, *CSF3* and *SST*, and of qPCR-verified DEGs, *IL1B* and *VGF*, and their interactions with other identified DEGs (*edgeR* $p<0.05$; no df) form a molecular network that can impair neuronal development, maintenance, survival, and function in DLPFC of LBD brains (Figure-1C). Furthermore, differential expression of *CSF3*, and of qPCR-verified DEGs, *IL1B*, *NOS3*, *VCAM1*, and *SPP1*, and their interactions with other identified DEGs form a molecular network that can lead to cell-to-cell signaling, and cellular movement impairment, immune system dysfunction, and neurodegeneration in ACC of LBD brains (Figure-1D).

Comparing with AD gene expression data:

We investigated whether the identified DEGs are specific to LBD or they represent a non-specific dementia phenotype by reviewing the AD-related gene expression data available in the NCBI GEO database (27). Downregulation of *RBM3* and *SST*, and upregulation of *GALNT6* in LBD were consistent with their differential expression levels, reported by prior AD studies. Differential expression levels of at least seven genome-wide significant DEGs (*SELE*, *CTSG*, *ALPI*, *ABCA13*, *CSF3*, *OXTR*, and *RAB44*) in LBD brains were distinct from their reported levels in AD brains (SDC-13).

Metabolic reprogramming in LBD brains:

The metabolic changes in the generated constraint-based flux balance LBD models (SDC-14) highlighted decreased mitochondrial respiratory chain activity by showing lower flux of tricarboxylic acid (TCA) cycle and oxidative phosphorylation for ATP-synthesis than those in NDC models. Reactive oxygen species (ROS), associated with neurodegeneration, were excessively produced in LBD reprogramed models. The glutathione peroxidase activity for scavenging ROS also was increased in the LBD reprogramed models, and the increased

flux for redox responses in LBD was dependent on NADPH-dependent hydrogen peroxide scavenging, catalyzed by isocitrate dehydrogenase (IDH) (Figure-2). IDH deficiency induces sensitivity to oxidative stress that leads to neurodegeneration (33), and the LBD reprogramed models showed high sensitivity to *in-silico* gene silencing of *IDH1* and *IDH2*. Moreover, the GEM demonstrated the importance of astrocytes releasing glutathione precursors. When we blocked astrocytes dependent reactions in the LBD models, the neurons could not handle the oxidative stress. Furthermore, we identified 84 reporter metabolites that displayed FDR-adjusted statistically significant changes in LBD brains (SDC-15). The downregulated reporter metabolites included those related to TCA cycle, such as malate, α-ketoglutarate, acetyl-CoA, NAD(H), acetate, glutamate, ubiquinone, estradiols, isobutyryl-CoA, and homocysteine, and several metabolites involved in fatty acids and lipid metabolism (SDC-14). These findings corroborated the lower flux of TCA cycle, and mitochondrial dysfunction in LBD brains (Figure-2).

Discussion:

Notwithstanding its small sample size, this is the hitherto largest RNA-Seq study investigating transcriptomics of LBD brains (13-15). Moreover, this is the first study evaluating the transcriptomic differences between DLB and PDD, and integrating LBD transcriptomic data into genome-scale metabolic modelling. We have identified 12 novel genome-wide significant DEGs, distinct from known genetic markers of AD and PD, in LBD brains, and have verified them using high-throughput qPCR. We identified specific dysfunctional molecular networks in LBD brains, and have added evidence for mitochondrial dysfunction and immunosenescence in LBD. The identified DEG, and their dysfunctional molecular networks advance molecular level mechanistic understanding of neurodegeneration in LBD, and they can facilitate identifying potential diagnostic biomarkers for LBD. Nevertheless, the

limitations of this study include its small sample size comprising mostly men, the lack of AD and PD comparison groups, not investigating cerebellum that does not typically have substantial α-synuclein pathology, and the lack of data on the use of dopaminergic medications.

Our GEM analyses have demonstrated how mitochondrial dysfunction and oxidative stress contribute towards neurodegeneration in LBD. Mitochondrial dysfunction can set off a vicious cycle by producing more ROS that lead to more mitochondrial oxidative damage (34). Consequent oxidative stress may lead to α-synuclein oligomerization worsening the vicious cycle by damaging more mitochondria (34). Oxidative stress has bidirectional causal relationship with hypoxia, and sustained hypoxia can lead to anti-inflammatory response in LBD brains (35). Moreover, the GEM demonstrated how astrocytes help neurons to cope with oxidative stress by releasing glutathione precursors. Hence, astrocytes dysfunction may contribute to neurodegeneration in LBD. Additionally, our findings indicate the need for further studies investigating IDH that catalyzes NADPH-dependent hydrogen peroxide scavenging as a potential therapeutic target that may modify the vicious cycle and the disease process.

Our results showed that the neuroimmunological profile of LBD brains differ widely from chronic neuroinflammation in AD (16). Prior evidence indicating neuroinflammation in LBD are weak, and they were principally derived from increased CD68 immunostaining that can be explained by impaired proteostasis and microglial dystrophy (17,18,36). Immunohistochemical staining with IBA1 and CD68 antibodies has demonstrated low microglia density, and increased microglial dystrophy in LBD brains (18). A recent transcriptomic and proteomic study has reported lack of evidence for microglia mediated neuroinflammation in post-mortem pulvinar of people with LBD (36). We have documented statistically significant downregulation of several cytokine and chemokine genes including *IL1B, IL2, IL6, CXCL2, CXCL3, CXCL8, CXCL10,* and *CXCL11*. Downregulation of *MPO,*

and of vascular cell adhesion molecules encoding *SELE* and *VCAM1* add evidence for the absence of neuroinflammation in LBD brains. Optimal microglial activation is essential for neuronal survival, and the importance of neuroprotective and synaptic modulatory functions of microglia in adult brain is increasingly recognized (37). Hence, immune dysfunction leading to impaired neuronal protection and survival rather than chronic neuroinflammation may explain neuronal loss in LBD. The differential expression levels of these inflammatory markers and of the associated molecules may distinguish LBD from AD, and further research investigating their biomarker potential are warranted.

Neutrophil extravasation has been associated with AD pathology (38), but little is known about its role in LBD. We have verified downregulation of neutrophil defensin genes, and have highlighted the dysfunctional granulocyte adhesion and diapedesis pathway in LBD brains. *CTSG* encoding a neutrophil serine protease, Cathepsin G, was significantly downregulated in both cortical regions of LBD brains. Cathepsin G influences the permeability of blood brain barrier, and its downregulation can contribute to impaired proteostasis and neurodegeneration in LBD (39). Moreover, Granulocyte colony stimulating factor (GCSF), coded by *CSF3*, stimulates the proliferation and survival of neutrophils and it is a neurotrophic factor (40). GCSF may facilitate neuroplasticity, and can inhibit apoptosis (41). We have documented *CSF3* downregulation in LBD brains, and have highlighted the importance of *CSF3* associated molecular networks hindering neuronal survival, and leading to immune dysfunction, and neurodegeneration in LBD. Serum GCSF levels were significantly less in people with AD than cognitively-intact controls (41), and a pilot study has demonstrated the safety of GCSF in people with AD (42). However, the biomarker and therapeutic potential of GCSF has not been systematically evaluated in LBD so far.

MPO polymorphisms have been associated with sporadic and familial forms of AD. Myeloperoxidase co-localizes with β-amyloid deposits in AD brains (43), and increased plasma

myeloperoxidase levels have been reported in people with AD (44). As we documented significantly reduced *MPO* expression in LBD, peripheral biomarker potential of myeloperoxidase and its mRNA in people with LBD warrant further investigation. Moreover, synaptic loss leads to neurodegeneration, and downregulation of *RBM3* reportedly leads to synaptic loss in mice (45). RBM3 modulates synaptic plasticity, and it can be a potential therapeutic target for LBD. Besides, our results rekindle the interest on somatostatinergic systems. Loss of somatostatin expressing interneurons (46), and consequent impairment of microglial migration and their target-specific phagocytosis (47) may contribute to cognitive impairment in LBD. Furthermore, downregulation of *VGF* may compromise neuronal survival and energy homeostasis in LBD brains. Increased expression of VGF in cerebrospinal fluid and peripheral lymphocytes has been detected in AD (48), but the biomarker potential of *VGF* has not been investigated in LBD.

As advanced stages of DLB and PDD are often clinically indistinguishable, the nosological validity and diagnostic boundaries of these disorders are continuously debated (49). We have documented the molecular differences between DLB and PDD, and more pronounced transcriptomic differences at earlier clinical stages can be hypothesized. Predicting early stage transcriptomic differences and their longitudinal changes from the findings of post-mortem brain studies are difficult. However, circulating exosomes transporting RNA between brain and peripheral systems provide an opportunity for studying the molecular changes in living human brain (50). Hence, we are currently investigating serum and cerebrospinal fluid exosomal RNA profiles for understanding the molecular changes in LBD over its disease course, and for evaluating the biomarker potential of identified DEGs.

Figure-legends:

Figure-1: Functional analyses of identified differentially expressed genes in post-mortem brains of people with Lewy body dementias

A: Canonical pathways that were enriched among the statistically significant (*edgeR* $p<0.05$; no df) differentially expressed genes (DEGs) in dorsolateral prefrontal cortices (DLPFC) of people with Lewy body dementias (LBD); B: Canonical pathways that were enriched among the statistically significant (*edgeR* $p<0.05$; no df) DEGs in anterior cingulate cortices (ACC) of people with LBD; (A&B) Green represents downregulated genes, and red represents upregulated genes. Yellow line presents the p-values after Benjamini-Hochberg false discovery rate (5%) correction.

C: A network of DEGs in DLPFC of people with LBD may impair neuronal development, maintenance, and survival; D: A network of DEGs in ACC of people with LBD may lead to cell-to-cell signaling impairment, and immune system dysfunction; (C&D) Green represents downregulated genes, and red represents upregulated genes. Solid lines represent direct interactions and dotted lines represent indirect interactions.

Figure-2: Flux balance analysis, performed on brain-specific genome scale metabolic models, highlighted the metabolic changes in LBD brains

The flux of reactions related to oxidative stress response increase in LBD. Scavenging of hydrogen peroxide (H_2O_2) is done by glutathione peroxidase. Astrocytes release the precursors of Glutathione (GSH). The increased flux for Redox responses to hypoxia in LBD is related to NADPH-dependent H_2O_2 scavenging, catalyzed by isocitrate dehydrogenase (IDH), supporting the system through the NADPH production. Additionally, the activity of tricarboxylic acid cycle and mitochondrial respiratory chain are reduced in LBD. aKG: alpha ketoglutarate, GSH: Reduced Glutathione and GSSG: Oxidized Glutathione.

Supplemental digital content (SDC):

1. SDC-1 presents the diagnosis, age, gender, post-mortem interval, and co-existent AD pathology of the brains that have been included in this study (.docx file).
2. SDC-2 presents the expression count matrix of RNA-seq data from post-mortem anterior cingulate cortices (.xlsx file).
3. SDC-3 presents the expression count matrix of RNA-seq data from post-mortem dorsolateral prefrontal cortices (.xlsx file).
4. SDC-4 presents forward and reverse primer sequences that have been used for high-throughput qPCR replication of 78 selected genes (first worksheet) and 7 reference (second worksheet) genes. It has two worksheets. (.xlsx file).
5. SDC-5 presents an overview of RNA extraction, cDNA synthesis, specific target amplification and high-throughput qPCR replication procedures (.docx file)
6. SDC-6 presents differential expression analyses of RNA-seq data from post-mortem anterior cingulate cortices of 13 Lewy body dementias, and 7 control brains without dementia and Parkinson's disease (.xlsx file).
7. SDC-7 presents differential expression analyses of RNA-seq data from post-mortem dorsolateral prefrontal cortices of 14 Lewy body dementias, and 6 control brains without dementia and Parkinson's disease (.xlsx file).
8. SDC-8 presents the results of high-throughput qPCR verification. It has two worksheets. First worksheet presents the results from anterior cingulate cortices, and the second worksheet presents the results from dorsolateral prefrontal cortices (.xlsx file).
9. SDC-9 presents differential expression analyses comparing post-mortem dementia with Lewy bodies and control brains without dementia and Parkinson's disease. It has two worksheets. First worksheet presents the results from anterior cingulate cortices, and the second worksheet presents the results from dorsolateral prefrontal cortices (.xlsx file).

10. SDC-10 presents differential expression analyses comparing post-mortem Parkinson's disease dementia and control brains without dementia and Parkinson's disease. It has two worksheets. First worksheet presents the results from anterior cingulate cortices, and the second worksheet presents the results from dorsolateral prefrontal cortices (.xlsx file).
11. SDC-11 presents differential expression analyses comparing post-mortem Parkinson's disease dementia and dementia with Lewy bodies brains. It has two worksheets. First worksheet presents the results from anterior cingulate cortices, and the second worksheet presents the results from dorsolateral prefrontal cortices (.xlsx file).
12. SDC-12 presents differential expression analyses comparing Lewy body dementia brains with minimal or no co-existing Alzheimer's disease pathology (All ABC scores ≤ 1) and Lewy body dementia brains with more co-existing Alzheimer's disease pathology (at least one of the ABC scores ≥ 2). It has two worksheets. First worksheet presents the results from anterior cingulate cortices, and the second worksheet presents the results from dorsolateral prefrontal cortices (.xlsx file).
13. SDC-13 presents differential expression fold changes, estimated by meta-analyses of prior gene expression studies investigating post-mortem Alzheimer's disease brains, of 26 selected differentially expressed genes in LBD (.xlsx file).
14. SDC-14 presents the flux balance analysis investigating the metabolic reprogramming in brains of people with Lewy body dementias. First worksheet presents the results from anterior cingulate cortices, and the second worksheet presents the results from dorsolateral prefrontal cortices (.xlsx file).
15. SDC-15 presents the reporter metabolite analysis investigating the metabolic reprogramming in brains of people with Lewy body dementias. It has six worksheets. The first three worksheets present the results from anterior cingulate cortices, and the next three worksheets present the results from dorsolateral prefrontal cortices (.xlsx file).

Acknowledgements:

This research was funded by the Biomedical Research Unit for Dementia (BRU-D) and the Maudsley Biomedical Research Centre (BRC) - dementia theme at the King's College London, London, UK. We thank the Brains for Dementia Research (BDR) network of brain banks for providing the necessary post-mortem brain tissues. The South West dementia brain bank, Bristol, UK, is a part of the BDR program, jointly funded by the Alzheimer's Research UK (ARUK) and the Alzheimer's Society, and is supported by the Bristol Research into Alzheimer's and Care of the Elderly, and the Medical Research Council (MRC), UK. We thank the donors whose donation of brain tissue to the London neurodegenerative diseases brain bank allowed this work to take place. The London brain bank is supported by the MRC and the BDR. The Manchester brain bank, a part of the BDR, receives service support costs from the MRC. The Newcastle brain tissue resource, another part of the BDR, is funded in part by a grant from the MRC (G0400074). We acknowledge the Oxford brain bank, supported by the MRC, the NIHR Oxford Biomedical Research Centre, and the BDR programme for providing post-mortem specimens. We thank the WHG that is funded in part by a Wellcome trust grant (reference: 203141/Z/16/Z). One of the authors (SS) is a recipient of fellowship from Engineering and Physical Sciences Research Council (EPSRC) and Biotechnology and Biological Sciences Research Council (BBSRC) (Project No. EP/S001301/1). The funding bodies did not play any role in the design, in the collection, analysis, and interpretation of data, and in the writing of the manuscript.

Funding source:

This research was funded by the Biomedical Research Unit for Dementia (BRU-D) and the Maudsley Biomedical Research Centre (BRC) - dementia theme at the King's College London, London, UK.

Author contributions:

APR, EC, AH, CB, PF, and DA were involved in the conception and the design of this research. APR, EC and PF obtained the post-mortem brain tissues, and extracted the RNA samples. APR, and GW analyzed the RNA-seq data, and completed subsequent functional analyses. GB, SS and AM analyzed the data using systems biology methods. APR, HM, and AH performed high-throughput qPCR replication and analyzed the data. APR, GB and SS drafted the initial manuscript. All authors were involved in the critical revisions and final approval of the manuscript.

Financial disclosures:

Prof. Dag Aarsland has received research support and/or honoraria from Astra-Zeneca, H. Lundbeck, Novartis Pharmaceuticals, and GE Health, and serves as paid consultant for H. Lundbeck, Eisai, and Axovant. Other authors do not have any competing interests to declare.

References:

1. Mayo MC,Bordelon Y: Dementia with Lewy bodies. Semin Neurol 2014; 34:182-188
2. Oesterhus R, Soennesyn H, Rongve A, et al: Long-term mortality in a cohort of home-dwelling elderly with mild Alzheimer's disease and Lewy body dementia. Dement Geriatr Cogn Disord 2014; 38:161-169
3. Vossius C, Rongve A, Testad I, et al: The use and costs of formal care in newly diagnosed dementia: a three-year prospective follow-up study. Am J Geriatr Psychiatry 2014; 22:381-388
4. Bougea A, Stefanis L, Paraskevas GP, et al: Neuropsychiatric symptoms and alpha-Synuclein profile of patients with Parkinson's disease dementia, dementia with Lewy bodies and Alzheimer's disease. J Neurol 2018; doi: 10.1007/s00415-00018-08992-00417. [Epub ahead of print]
5. Freer J: UK lags far behind Europe on diagnosis of dementia with Lewy bodies. BMJ 2017; 358:j3319
6. Schade S,Mollenhauer B: Biomarkers in biological fluids for dementia with Lewy bodies. Alzheimers Res Ther 2014; 6:72
7. Walker Z, Possin KL, Boeve BF, et al: Lewy body dementias. Lancet 2015; 386:1683-1697
8. Velayudhan L, Ffytche D, Ballard C, et al: New Therapeutic Strategies for Lewy Body Dementias. Curr Neurol Neurosci Rep 2017; 17:68
9. Guerreiro R, Ross OA, Kun-Rodrigues C, et al: Investigating the genetic architecture of dementia with Lewy bodies: a two-stage genome-wide association study. Lancet Neurol 2018; 17:64-74
10. Keogh MJ, Kurzawa-Akanbi M, Griffin H, et al: Exome sequencing in dementia with Lewy bodies. Transl Psychiatry 2016; 6:e728
11. Bras J, Guerreiro R, Darwent L, et al: Genetic analysis implicates APOE, SNCA and suggests lysosomal dysfunction in the etiology of dementia with Lewy bodies. Hum Mol Genet 2014; 23:6139-6146

12. McKeith IG, Boeve BF, Dickson DW, et al: Diagnosis and management of dementia with Lewy bodies: Fourth consensus report of the DLB Consortium. Neurology 2017; 89:88-100
13. Santpere G, Garcia-Esparcia P, Andres-Benito P, et al: Transcriptional network analysis in frontal cortex in Lewy body diseases with focus on dementia with Lewy bodies. Brain Pathol 2018; 28:315-333
14. Henderson-Smith A, Corneveaux JJ, De Both M, et al: Next-generation profiling to identify the molecular etiology of Parkinson dementia. Neurol Genet 2016; 2:e75
15. Pietrzak M, Papp A, Curtis A, et al: Gene expression profiling of brain samples from patients with Lewy body dementia. Biochem Biophys Res Commun 2016; 479:875-880
16. Calsolaro V,Edison P: Neuroinflammation in Alzheimer's disease: Current evidence and future directions. Alzheimers Dement 2016; 12:719-732
17. Streit WJ,Xue QS: Microglia in dementia with Lewy bodies. Brain Behav Immun 2016; 55:191-201
18. Bachstetter AD, Van Eldik LJ, Schmitt FA, et al: Disease-related microglia heterogeneity in the hippocampus of Alzheimer's disease, dementia with Lewy bodies, and hippocampal sclerosis of aging. Acta Neuropathol Commun 2015; 3:32
19. Howlett DR, Whitfield D, Johnson M, et al: Regional Multiple Pathology Scores Are Associated with Cognitive Decline in Lewy Body Dementias. Brain Pathol 2015; 25:401-408
20. Kovari E, Gold G, Herrmann FR, et al: Lewy body densities in the entorhinal and anterior cingulate cortex predict cognitive deficits in Parkinson's disease. Acta Neuropathol 2003; 106:83-88
21. Bronnick K, Breitve MH, Rongve A, et al: Neurocognitive Deficits Distinguishing Mild Dementia with Lewy Bodies from Mild Alzheimer's Disease are Associated with Parkinsonism. J Alzheimers Dis 2016; 53:1277-1285

22. Kim D, Langmead B,Salzberg SL: HISAT: a fast spliced aligner with low memory requirements. Nat Methods 2015; 12:357-360
23. Liao Y, Smyth GK,Shi W: featureCounts: an efficient general purpose program for assigning sequence reads to genomic features. Bioinformatics 2014; 30:923-930
24. Rajkumar AP, Qvist P, Lazarus R, et al: Experimental validation of methods for differential gene expression analysis and sample pooling in RNA-seq. BMC Genomics 2015; 16:548
25. Anders S, McCarthy DJ, Chen Y, et al: Count-based differential expression analysis of RNA sequencing data using R and Bioconductor. Nat Protoc 2013; 8:1765-1786
26. Leek JT, Taub MA,Rasgon JL: A statistical approach to selecting and confirming validation targets in -omics experiments. BMC Bioinformatics 2012; 13:150
27. Barrett T, Wilhite SE, Ledoux P, et al: NCBI GEO: archive for functional genomics data sets--update. Nucleic Acids Res 2013; 41:D991-995
28. Sertbas M, Ulgen K,Cakir T: Systematic analysis of transcription-level effects of neurodegenerative diseases on human brain metabolism by a newly reconstructed brain-specific metabolic network. FEBS Open Bio 2014; 4:542-553
29. Jensen PA,Papin JA: Functional integration of a metabolic network model and expression data without arbitrary thresholding. Bioinformatics 2011; 27:541-547
30. Jensen PA, Lutz KA,Papin JA: TIGER: Toolbox for integrating genome-scale metabolic models, expression data, and transcriptional regulatory networks. BMC Syst Biol 2011; 5:147
31. Bidkhori G, Benfeitas R, Elmas E, et al: Metabolic Network-Based Identification and Prioritization of Anticancer Targets Based on Expression Data in Hepatocellular Carcinoma. Front Physiol 2018; 9:916
32. Varemo L, Nielsen J,Nookaew I: Enriching the gene set analysis of genome-wide data by incorporating directionality of gene expression and combining statistical hypotheses and methods. Nucleic Acids Res 2013; 41:4378-4391

33. Kim H, Kim SH, Cha H, et al: IDH2 deficiency promotes mitochondrial dysfunction and dopaminergic neurotoxicity: implications for Parkinson's disease. Free Radic Res 2016; 50:853-860
34. Spano M, Signorelli M, Vitaliani R, et al: The possible involvement of mitochondrial dysfunctions in Lewy body dementia: a systematic review. Funct Neurol 2015; 30:151-158
35. Taylor CT,Colgan SP: Regulation of immunity and inflammation by hypoxia in immunological niches. Nat Rev Immunol 2017; 17:774-785
36. Erskine D, Ding J, Thomas AJ, et al: Molecular changes in the absence of severe pathology in the pulvinar in dementia with Lewy bodies. Mov Disord 2018; 33:982-991
37. Chen Z, Jalabi W, Hu W, et al: Microglial displacement of inhibitory synapses provides neuroprotection in the adult brain. Nat Commun 2014; 5:4486
38. Zenaro E, Pietronigro E, Della Bianca V, et al: Neutrophils promote Alzheimer's disease-like pathology and cognitive decline via LFA-1 integrin. Nat Med 2015; 21:880-886
39. Stoka V, Turk V,Turk B: Lysosomal cathepsins and their regulation in aging and neurodegeneration. Ageing Res Rev 2016; 32:22-37
40. Prakash A, Medhi B,Chopra K: Granulocyte colony stimulating factor (GCSF) improves memory and neurobehavior in an amyloid-beta induced experimental model of Alzheimer's disease. Pharmacol Biochem Behav 2013; 110:46-57
41. Barber RC, Edwards MI, Xiao G, et al: Serum granulocyte colony-stimulating factor and Alzheimer's disease. Dement Geriatr Cogn Dis Extra 2012; 2:353-360
42. Sanchez-Ramos J, Cimino C, Avila R, et al: Pilot study of granulocyte-colony stimulating factor for treatment of Alzheimer's disease. J Alzheimers Dis 2012; 31:843-855
43. Green PS, Mendez AJ, Jacob JS, et al: Neuronal expression of myeloperoxidase is increased in Alzheimer's disease. J Neurochem 2004; 90:724-733
44. Tzikas S, Schlak D, Sopova K, et al: Increased myeloperoxidase plasma levels in patients with Alzheimer's disease. J Alzheimers Dis 2014; 39:557-564

45. Peretti D, Bastide A, Radford H, et al: RBM3 mediates structural plasticity and protective effects of cooling in neurodegeneration. Nature 2015; 518:236-239

46. Flores-Cuadrado A, Ubeda-Banon I, Saiz-Sanchez D, et al: alpha-Synucleinopathy in the Human Amygdala in Parkinson Disease: Differential Vulnerability of Somatostatin- and Parvalbumin-Expressing Neurons. J Neuropathol Exp Neurol 2017; 76:754-758

47. Fleisher-Berkovich S, Filipovich-Rimon T, Ben-Shmuel S, et al: Distinct modulation of microglial amyloid beta phagocytosis and migration by neuropeptides (i). J Neuroinflammation 2010; 7:61

48. Busse S, Steiner J, Glorius S, et al: VGF expression by T lymphocytes in patients with Alzheimer's disease. Oncotarget 2015; 6:14843-14851

49. Postuma RB, Berg D, Stern M, et al: Abolishing the 1-year rule: How much evidence will be enough? Mov Disord 2016; 31:1623-1627

50. Janas AM, Sapon K, Janas T, et al: Exosomes and other extracellular vesicles in neural cells and neurodegenerative diseases. Biochim Biophys Acta 2016; 1858:1139-1151

Figure 1

Click here to access/download;Figure;Figure 1.jpeg

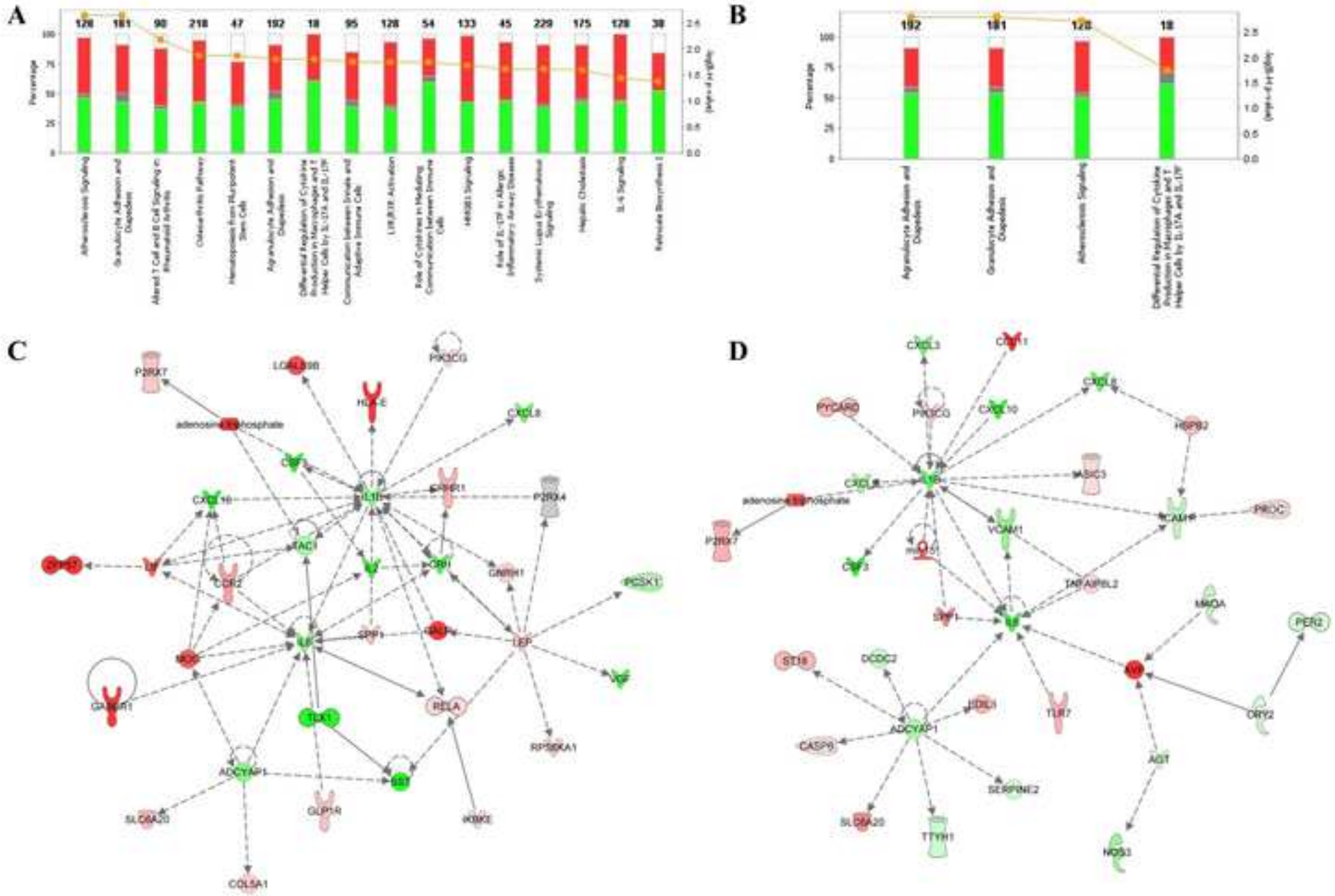

Figure 2

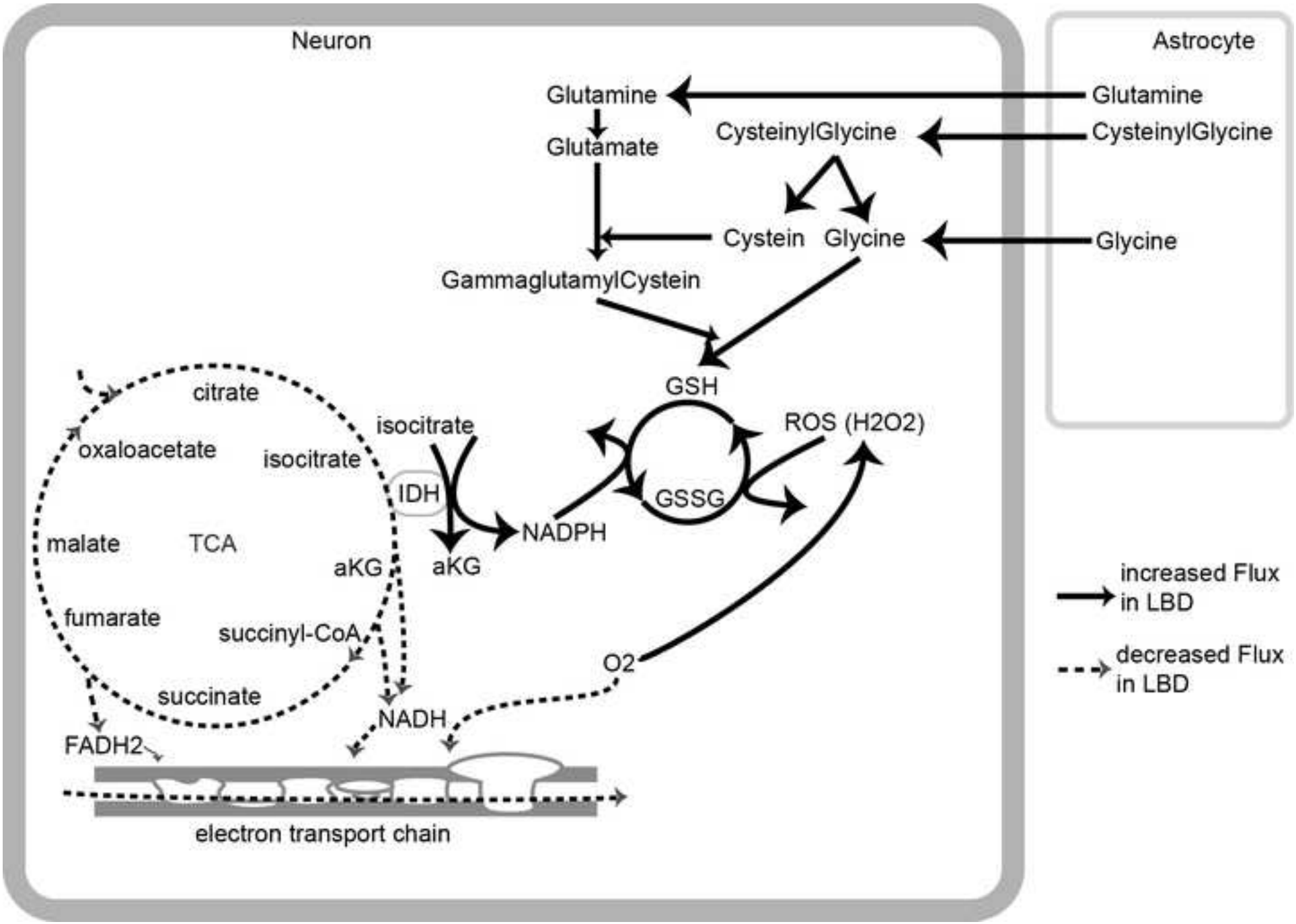

Table 1: 12 genome-wide significant differentially expressed genes[a] in post-mortem brains of people with Lewy body dementias

Gene	Gene name	LFC [b]	qPCR LFC	p [c]	q [d]
MPO	myeloperoxidase	-4.49	-3.58	5.43E-11	3.07E-06
SELE	selectin E	-3.64	-2.47	2.90E-09	8.19E-05
ABCA13	ATP binding cassette subfamily A member 13	-3.63	-2.36	8.85E-08	0.0017
ALPI	alkaline phosphatase, intestinal	-6.69	-1.17	4.36E-07	0.0054
SLC4A1	solute carrier family 4 member 1	-2.61	-1.55	4.80E-07	0.0054
OXTR	oxytocin receptor	-1.08	-0.94	6.93E-07	0.0065
CSF3	colony stimulating factor 3	-4.14	-5.57	9.06E-07	0.0073
CTSG	cathepsin G	-6.75	-7.61	4.56E-06	0.0286
RAB44	RAB44, member RAS oncogene family	-3.88	-1.92	4.26E-06	0.0286
RBM3	RNA binding motif protein 3	-1.03	-2.17	5.74E-06	0.0303
GALNT6	polypeptide N-acetylgalactosaminyltransferase 6	1.35[e]	0.95[e]	4.33E-07	0.0049
SST	somatostatin	-2.27[e]	-1.61[e]	8.89E-07	0.0072

[a] Differentially expressed genes that were identified by RNA-seq and were verified by high-throughput quantitative polymerase chain reaction (qPCR); [b] Logarithmic (base 2) fold change, measured by RNA-seq; [c] RNA-seq p value that was estimated using the edgeR algorithm. The *edgeR* algorithm employed exact tests (no df) for calculating p-values after fitting gene-specific quasi-negative binominal models and estimating dispersion using the quantile adjusted conditional maximum likelihood method; [d] RNA-seq q value after Benjamini-Hochberg false discovery rate (5%) correction; [e] in dorsolateral prefrontal cortex.

Table 2: Other verified differentially expressed genes [a] in post-mortem brains of people with Lewy body dementias

Anterior Cingulate Cortex					Dorsolateral Prefrontal Cortex				
Gene	**LFC [b]**	**qPCR LFC**	**p [c]**	**q [d]**	**Gene**	**LFC [b]**	**qPCR LFC**	**p [c]**	**q [d]**
ADAMTS2	1.05	1.23	1.15E-05	0.0521	*CXCL11*	-3.72	-2.35	1.14E-05	0.0682
UTF1	-3.73	-1.53	1.22E-05	0.0521	*VGF*	-1.79	-0.79	4.73E-05	0.2058
DEFA4	-6.15	-2.37	2.91E-05	0.0897	*ADAMTS2*	1.02	2.15	0.0001	0.3372
CXCL11	-3.19	-1.91	7.43E-05	0.1399	*LDHC*	4.16	5.49	0.0002	0.4165
XIST	8.56	1.43	0.0002	0.2581	*GIPR*	2.30	1.18	0.0004	0.4165
DEFA3	-5.34	-2.64	0.0004	0.3266	*XIST*	8.75	1.83	0.0006	0.4652
GBP6	-1.18	-2.52	0.0013	0.4438	*ADRA2B*	1.48	-0.86	0.0009	0.5467
STX11	-1.24	-1.03	0.0015	0.4701	*DEFA4*	-4.95	-3.91	0.0010	0.5467
GRK7	1.64	2.01	0.0015	0.4725	*GBP6*	-1.42	-1.30	0.0015	0.6017
GIPR	1.60	0.84	0.0020	0.4911	*REG4*	-4.15	-1.19	0.0019	0.6017
ABCD2	-0.59	-0.70	0.0020	0.4911	*SBSN*	1.84	0.39	0.0036	0.7670
IL1B	-1.68	-1.49	0.0050	0.6213	*DEFA3*	-3.77	-2.62	0.0076	0.8123
SPP1	1.40	0.95	0.0053	0.6213	*SPP1*	0.96	0.80	0.0102	0.8329
VCAM1	-1.18	-1.32	0.0124	0.7229	*IL1B*	-1.41	-1.01	0.0103	0.8335
VGF	-0.91	-2.64	0.0230	0.7684	*CPA3*	-3.77	-2.17	0.0142	0.8849
CP	-0.93	-1.12	0.0257	0.7764	*GRK7*	1.24	1.97	0.0201	0.9649
CRABP1	1.57	0.78	0.0265	0.7767	*WISP1*	1.11	1.11	0.0275	1.0000
LDHC	2.37	2.78	0.0395	0.8274	*CP*	-0.91	-1.34	0.0277	1.0000
NOS3	-1.08	-1.20	0.0454	0.8274	*GPR50*	-2.04	-1.93	0.0412	1.0000
OR11H4	-1.26	-1.35	0.0471	0.8274	*ABCD2*	-0.43	-0.57	0.0463	1.0000

[a] Differentially expressed genes that were identified by RNA-seq and were verified by high-throughput qPCR; [b] Logarithmic (base 2) fold change, measured by RNA-seq; [c] RNA-seq p value that was estimated using *edgeR* algorithm. The *edgeR* algorithm employed exact tests (no df) for calculating p-values after fitting gene-specific quasi-negative binominal models and estimating dispersion using the quantile adjusted conditional maximum likelihood method; [d] RNA-seq q value after Benjamini-Hochberg false discovery rate (5%) correction.